Numerical analysis of the dispersion of acoustic Rayleigh waves in a Functionally Graded Piezoelectric half-Space

Loukmane El Khaldi* and *Mustapha* Sanbi

Team of Advanced Sciences and Technologies, ENSA Tetouan, Abdelmalek Essaadi University, Tetouan, Morocco

Abstract. Considerable attention has been given to the study of the propagation of surface waves in order to improve the efficiency and lifetime of the surface acoustic wave devices such as transducers. In this paper, an investigation of the Rayleigh waves in functionally graded piezoelectric material is presented. The Rayleigh surface wave propagation is assumed to take place in a transversely isotropic graded piezoelectric half-space with material properties varying continuously along the thickness direction. The obtained results have shown that dispersive Rayleigh waves can propagate on the surface of the FGPM half-space with characteristics that depend on the graded variation of the material parameters. Based on the dispersion relations, the phase velocity for both the electrically open and shorted cases at the free surface is deduced. The displacement magnitudes and the corresponding decay variations are plotted and discussed.

1 Introduction

Several studies have been dedicated to the propagation of transverse surface waves in inhomogeneous half-space or in multilayer structures [1-2]. Other works have been carried out on Rayleigh waves (RW) that propagate in hetero-structures composed of a film deposited on an isotropic homogeneous substrate and having properties that vary continuously in the thickness direction [3].

Sanbi et al. [4] analyzed the effects of thermal and centrifugal acceleration on the propagation of acoustic waves taking place in a half-space thermo-piezo-electric material surface. This was performed under the assumptions of linear thermo-piezo-electricity and included centrifugal and Coriolis forces. Cao et al. [5] studied the dispersive behavior of RW in a half-space by using the perturbation technique. Li et al. [6] investigated RW propagation in a Functionally Graded Piezoelectric Material (FGPM) half-space by means of a method based on the Laguerre polynomials. Zhang et al. [7] used an exact approach to investigate RW in an initially stressed Magneto-Electro-Elastic half-space. Narendar et al. [8] used the nonlocal continuum theory to study the effect of temperature on the propagation of ultrasonic waves in a nanoplate. Dammak et al. [9] analyzed the propagation of Lamb wave in an FGPM. Ezzin et al. [10] solved the dynamic ordinary differential equations that govern the propagation of waves taking place in a semi-infinite substrate having piezo-magnetic properties and covered with an FGPM layer.

The present work focuses on studying the effects of temperature and rotation affecting the RW dispersive curves in the case of a thermo-piezo-electric half-space having piezo-electric gradient material (PGM) propriety. The equation of motion, the constitutive equations of linear thermo-piezo-electricity and the temperature equation are formulated. During propagation, the plate surfaces are considered rotating around a threefold axis of symmetry, free of any stress, thermally isolated and electrically short-circuited/charge-free. The half-space is cut along a plane normal to one of these axes. The explicit equations are derived for both non-rotating and rotating cases, with the surface conditions being either open or short circuits. The effects on the RW due to initial temperature of the medium, imposed rotation and pyro-electric properties are studied and discussed.

2 Theoretical study

2.1 Problem statement

In the following, the propagation of RW is studied numerically in a system consisting of a ceramic film of zirconate and lead titanate PZT-6B, having FGPM properties and thickness h, see in Fig.1. It is assumed that this structure can be considered as a layered piezo-electric half-space system. The equations related to the fundamental relation of dynamics and Hooke's law will be developed in a coordinate system denoted (x, y, z) in which the plane (x, z) is taken parallel to the RW wave polarization. The (x, y) plane represents the free surface $z = 0$, and the guiding direction merges with the x axis. To retrieve piezo-active Rayleigh mode waves, the symmetry axis of the PZT is taken parallel to the propagation direction x. The mechanical and electrical properties of the FGPM film are considered to vary

* Corresponding author: loukmane.elkhaldi@gmail.com

continuously with thickness. The body is assumed to rotate around the z axis, at a constant velocity rate Ω.

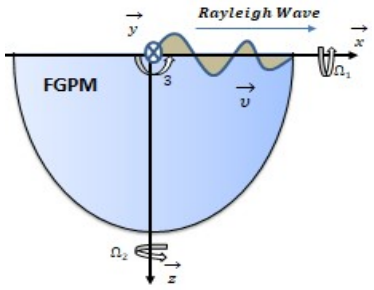

Fig. 1. The FGPM half-space and the coordinates system.

2.2 Governing equations of the problem

The theory of nonlocal elasticity is a framework which considers, at a given location, the relative influences on the stress which are due to deformations occurring at the vicinity of this location. The equations of motion, Coulomb's law and Maxwell's equation, for a nonlocal linear elastic solid, as given in [11], write:

$$T_{ij,j} + f_i = \rho \ddot{u}_i \,,\; D_{i,i} = 0 \,,\; E_i = -\phi_{,i} \tag{1}$$

where ρ is the mass density, T_{ij} are the stress tensor terms, f_i the mechanical body force components and u_i the mechanical displacements and ϕ the potential.

In the absence of a surface heat source, the equations describing linear thermo-piezo-electricity and heat transfer under small deformation assumption write:

$$T_{ij} = C_{ijkl} S_{kl} - e^{T}_{kij} E_k - \lambda_{ij} \theta \tag{2}$$

$$D_j = e_{jkl} S_{kl} + \varepsilon_{jk} E_k + p_i \theta \tag{3}$$

$$\left(\frac{\rho c_0}{\theta_0} \right) \dot{\theta} + \lambda_{ij} \dot{S}_{ij} + p_i \dot{E}_i = -\kappa_{ij} \theta_{,ij} \tag{4}$$

where $\mathbf{S}$ is the strain tensor, $\mathbf{E}$ electric field, $\mathbf{D}$ dielectric displacement, θ temperature variation, c_0 the specific heat per unit mass, θ_0 the initial temperature, $\mathbf{C}$ the elastic tensor. The quantities $\mathbf{e}$, $\boldsymbol{\varepsilon}$, $\boldsymbol{\lambda}$, $\boldsymbol{\kappa}$ and $\mathbf{p}$ are respectively, piezo-electric, dielectric, thermal coefficients, thermal conductivities and pyro-electric tensors. The superscript T in $\mathbf{e}$ designates transpose.

The strain components are related to the mechanical displacements by the following equations:

$$2S_{ij} = u_{i,j} + u_{j,i} \tag{5}$$

The existence of coupled RW that propagate at the surface of FGPM half-space is investigated in the subsequent under the assumption of wave propagation in the positive direction of the x-axis, with no displacement along y-axis. The expected RW wave is taken under the form

$$u_x = u_x(x,z,t) \,, u_y = 0 \;\; , u_z = u_z(x,z,t) \,, \phi = \phi(x,z,t) \tag{6}$$

2.3 Implementation for an FGPM

Taking the density ρ to be practically constant and neglecting temperature variation, Adler [12] has given, for a homogeneous system along the z direction, the acoustic fundamental tensor in the form of sub-matrices Γ_{ik} as follows:

$$\Gamma_{ik} = \begin{bmatrix} C_{1i1k} & C_{1i2k} & C_{1i3k} & e_{k1i} \\ C_{2i1k} & C_{2i2k} & C_{2i3k} & e_{k2i} \\ C_{3i1k} & C_{3i2k} & C_{3i3k} & e_{k3i} \\ e_{i1k} & e_{i2k} & e_{i3k} & -\varepsilon_{ik} \end{bmatrix} i,k = 1,3 \tag{7}$$

Here, the piezoelectric layer depicted in Fig.1 is assumed to have material properties that vary according to exponential gradient distributions along the z-axis. The coupling effect of temperature and electrical and mechanical parameters is considered separately. It should be noticed that even if these distributions of material constants are not necessarily realistic, they will allow for more understanding of the influence of the material gradient on the wave propagation characteristics. The purpose is to improve design of more efficient devices in practice.

The elastic stiffness constants C_{ijkl} $(i,j,k,l = 1,2,3)$ are usually reduced to 36 constants and can be taken through using the Voigt notations as C_{pq} $(p,q = 1,...,6)$. The material properties corresponding to elastic, piezo-electric and electrical properties that are used in the following are: $C_{11} = 168GPa$, $C_{12} = 60GPa$, $C_{44} = 27.1GPa$, $C_{33} = 163GPa$, $C_{66} = 54GPa$, $e_{31} = -0.9C.m^{-2}$, $e_{33} = 7.1C.m^{-2}$, $e_{15} = 4.6C.m^{-2}$, $\varepsilon_{11} = 3.6nF.m^{-1}$, $\varepsilon_{33} = 3.4nF.m^{-1}$, $\rho = 7800kg.m^{-3}$, $c_0 = 420J.kg^{-1}.K^{-1}$, $\lambda_{11} = \lambda_{22} = 2.016MPa.K^{-1}$, $\kappa_{11} = \kappa_{22} = 1.2W.m^{-1}.K^{-1}$, $p_3 = 37kC.K^{-1}.m^{-2}$

2.4 Prescribed boundary conditions

To determine a RW propagating at the surface of an FGPM, sufficient mechanical and electrical boundary conditions have to be prescribed. The electrical boundary conditions correspond to either electrically open or shorted circuits. Both of them are considered in this study. For a wave that propagates along an electroded surface, $z = 0$, which is free from any mechanical loads, the following boundary conditions hold:

$$T_{12} = T_{22} = T_{32} = 0 \,, \phi = 0 \,, \theta = 0 \,, \sigma = 0 \tag{8}$$

where σ denotes the electric charge density. This is deduced from the continuity relation of D_3 as:

$$\sigma = D_3(-h^+) - D_3(-h^-) \tag{9}$$

Assuming that the half-space material is homogeneous, a surface wave that propagates along the x-axis is searched under the following form:

$$\begin{bmatrix} u_{1,2,3} \\ \theta \end{bmatrix} = \begin{bmatrix} A_{1,2,3} \\ A_4 \end{bmatrix} e^{k\eta z} e^{ik(x-vt)}, \quad \phi = iA_5 e^{kz} e^{ik(x-vt)} \qquad 10)$$

where i is the unit imaginary number, ω the frequency, k the wave number, v the phase velocity and $A_.$ are amplitudes. A_5 is taken real, while A_j, A_4 are complex. The frequency and the wave number are positive and verify the relation: $\omega = kv$.

3 Surface waves solutions

Substituting the expressions in Eq. (10) into Eq. (1) leads to the following complex eigenvalue problem:

$$a_{ij} A_j = 0 \qquad (11)$$

with $a_{11} = v_2^2\eta^2 - v_1^2 + v^2\left(1+\Omega^2/\omega^2\right)$, $a_{12} = i\eta(v_1^2 - v_2^2)$, $a_{14} = i\alpha$, $a_{22} = v_1^2\eta^2 - v_2^2 + v^2$, $a_{23} = 0$, $a_{24} = i\alpha\eta$, $a_{13} = 2iv^2\Omega/\omega$, $a_{31} = -a_{13}$, $a_{32} = 0$, $a_{33} = v_3^2(\eta^2 - 1) + v^2\left(1+\Omega^2/\omega^2\right)$, $a_{34} = 0$, $a_{44} = i\beta_0 + \beta$ in which $\alpha = -\lambda_{11}/(k\rho)$, $\beta_0 = \rho c_0/(\theta_0 k^2)$, $\beta = \kappa(\eta^2 - 1)/(kv)$, $v_1^2 = C_{11}/\rho$, $v_2^2 = C_{66}/\rho$, $v_3^2 = \overline{C}_{44}/\rho$ where $C_{66} = (C_{11} - C_{12})/2$, $\overline{C}_{44} = C_{44} - (e_{15}^2/\varepsilon_{11})$.

Eq. (11) shows that for $\Omega \neq 0$, the phase velocity v and the frequency ω are generally nonlinearly dependent. This means that the rotation effect yields, generally, to dispersive surface waves. As the ratio Ω/ω is small, the forces are found to be of the same order than this parameter. They depend also upon the thermal and physical material properties.

Solution of Eq. (11) can be obtained under the following form:

$$\begin{bmatrix} u_{1,2,3} \\ \theta \end{bmatrix} = \sum_{j=1}^{4} c_j \begin{bmatrix} A_{1,2,3}^j \\ A_4 \end{bmatrix} e^{k\eta_j z} e^{ik(x-vt)}$$
$$\phi = ic_5 e^{kz} e^{ik(x-vt)} \qquad (12)$$

where A^j is the eigenvector associated to the eigenvalue η_j^2. The constants c_j and c_5 represent respectively the complex and real magnitudes that are still to be determined. Substituting Eq. (12) into Eq. (8) yields the following eigenvalue equation:

$$b_{ij} c_j = 0 \qquad (13)$$

with $b_{1j} = \eta_j A_1^j + iA_2^j$, $b_{2j} = ic_{12}A_1^j + c_{11}\eta_j A_2^j - \lambda_{11}A_5^j/\kappa$, $b_{15} = 0$, $b_{25} = b_{52} = 0$, $b_{3j} = \overline{c}_{44}\eta_j A_3^j$, $b_{35} = e_{15}$, $b_{4j} = e_{15}A_3^j$, $b_{45} = \varepsilon_{11}$, $b_{51} = A_4^1$, $b_{54} = A_4^4$, $b_{53} = b_{55} = 0$.

4 Results and discussions

Considering the thermo-piezo-electric ceramic PZT-6B, numerical simulations were performed in order to illustrate the effects resulting from thermo-mechanical coupling, preheating temperature and body rotation. These effects are studied for a generalized RW propagating along the x direction. The results are given in terms of the linear dispersion spectra, and the profiles of the longitudinal mechanical displacements versus the z coordinate. They were obtained by taking into account small or large ratios for the rotation of thermo-piezo-electric body, and also with considering or not the centrifugal accelerations. The dispersion curves are plotted for various initial temperatures.

Considering a material electroded surface, Fig. 2 gives RW phase velocity as a function of $(\Omega_{1,2,3}/\omega)$ rotations about the three-symmetry axis. Fig.3 presents RW velocity versus large rotation ratios $(\Omega_{1,2,3}/\omega)$ about the three-symmetry axis for two values of the initial temperature: $30°C$ and $50°C$. For an electroded surface of the material, Fig. 4 gives the changes of wave velocity for different initial body temperatures θ_0 and $(\Omega_{1,2,3}/\omega)$ rotation ratios about the three-symmetry axis.

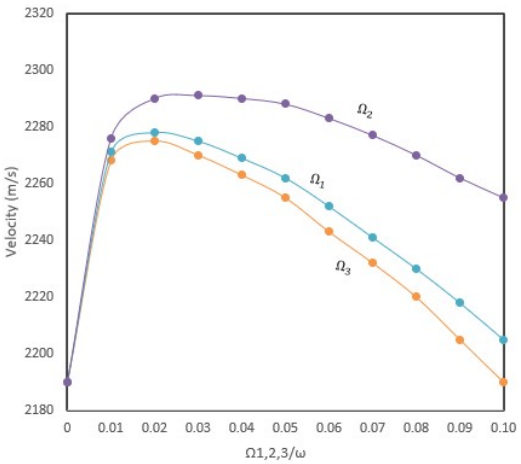

Fig.2. Phase velocity of RW versus rotation ratios $(\Omega_{1,2,3}/\omega)$ for an electroded surface.

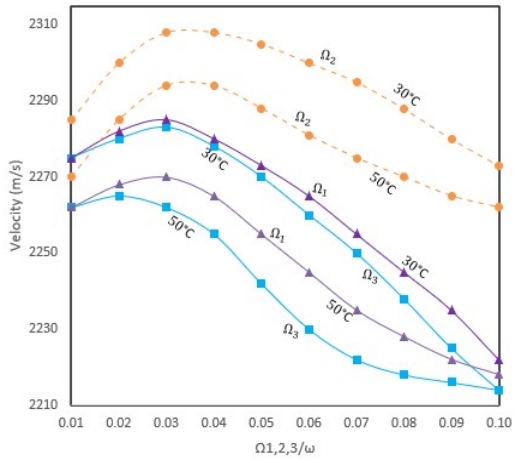

Fig. 3. Phase velocity of RW versus $(\Omega_{1,2,3}/\omega)$ for an electroded surface and initial temperatures $30°C$ and $50°C$.

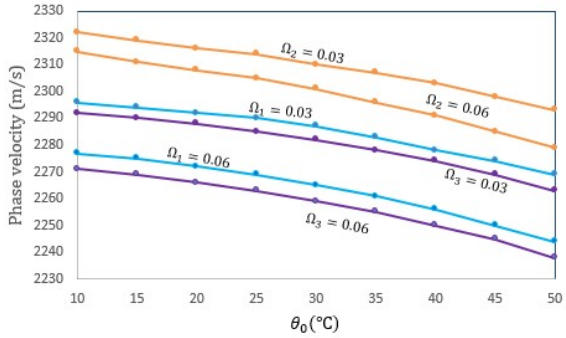

Fig.4. Rayleigh wave velocity versus preheating temperatures of the body θ_0 with ratios $(\Omega_{1,2,3}/\omega)$

Fig. 1 and Fig. 2 show that temperature and rotation velocity have an important effect on phase velocity. As shown in Fig. 3, an abnormal dispersion occurs when the rate is small $(\Omega/\omega < 0.033)$ as the velocity of RW increases locally for increasing values of rotation rate. This behaviour of the dispersive curves may be attributed to the coupling effect resulting in the studied material from temperature, piezo-electricity and pyro-electricity. Besides, the RW phase velocity decreases for increasing initial temperature, except for small values of rotation ratio for which the wave speed is increasing.

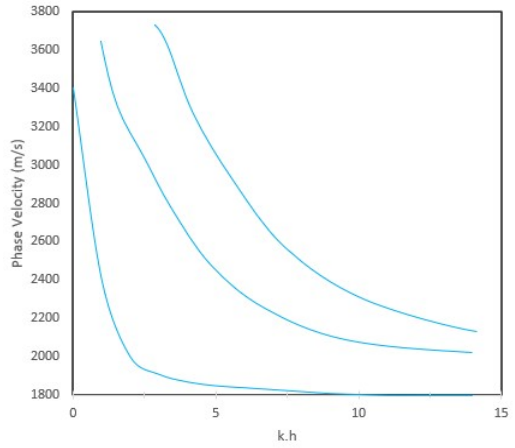

Fig.5. RW velocity of the first three modes for the short-circuit FGPM structure.

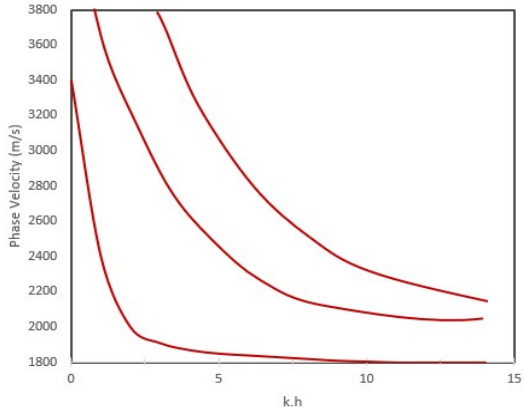

Fig.6. RW velocity of the first three modes for the open circuit FGPM structure.

The phase velocity of RW is now calculated for the case of an FGPM. The considered frequency interval goes up to the value $50MHz$. The associated product wavenumber × thickness is $kh = 15$. The obtained first three modes of RW in shorted circuit and open circuit polarization are given respectively in Fig.5 and Fig.6. From these figures, one can see that the RW velocity depends more on the frequency below $kh = 5$. The dispersion curves show a large velocity gap in the gradient structure. Therefore, the profile of the dispersion curves for the first three modes confirms that the thermal effect should not be neglected as it can influence significantly the propagation of waves.

5 Conclusions

In this work, propagation of the Rayleigh surface waves in a layer of functionally gradient piezo-electric material was studied by using a matrix based numerical method. Solution in terms of the dispersion curves of the coupled thermo-piezo-electric equations was obtained analytically for both the conditions of electrically open and short circuits. The obtained results have shown that Rayleigh waves are generally spin-dispersive. Certain abnormal dispersions were observed for small rotations: wave speed increases locally when the rotation ratio increases. It was found that the effect of the gradient resulting from the physical properties sensitivity to the deposition temperature is important. The simulations have shown also that the electro-mechanical and pyro-electric couplings influence the dispersion curves.

References

1. Z.H. Qian, F. Jin, T. Lu, K. Kishimoto, Smart Mater. Struct. **17** (2008)
2. B. Collet, M. Destrade, G.A. Maugin, Eur. J. Mech. A/Solids **25** (2006)
3. Z.H. Qian, F. Jin, Z. Wang, K. Kishimoto, Acta Mech. **171** (2004)
4. M. Sanbi, M. El Marhoune, E.H. Essoufi, L.A. Faik, M. Rahmoune, Int. J. Mech. Mechatr. Eng. **16** (2016)
5. X. Cao, F. Jin, Z. Wang, Acta Mech. **200** (2008)
6. K. Li, S. Jing, J. Yu, X. Zhang, B. Zhang, Materials **13**, 10 (2020)
7. R. Zhang, Y. Pang, W. Feng, Mech. Adv. Mater. Struct. **21** (2014)
8. S. Narendar, S. Gopalakrishnan, Compos. Part B Eng. **43** (2012)
9. Y. Dammak, J.H. Thomas, M.H.B. Ghozlen, Phys. Procedia **70** (2015)
10. H. Ezzin, M. Mkaoir, M. Ben Amor, Superlattices Microstruct. **112** (2017)
11. F. Benmeddour, S. Grondel, J. Assaad, E. Moulin, Ultrasonics **49** (2009)
12. E.L. Adler, IEEE Trans. Ultrason. Ferroelectr. Freq. Control **41** (1994)